DOI:
10.1161/CIRCEP.117.005897

Document Version
Peer reviewed version

Unravelling the Underlying Arrhythmia Mechanism in Persistent AF – Results from the Signal Transfer of AtRiaL fIbrillation to Guide Human Treatment (STARLIGHT)

Running title: *Child et al.; Understanding the Arrhythmia mechanism in PsAF*

Nicholas Child, BM[1]; Richard H. Clayton, PhD[2]; Caroline Roney, PhD[1]; Jacob Laughner, PhD[3]; Allan Shuros, MS[3]; Petr Neuzil, MD[4]; Jan Petru, MD[4]; Tom Jackson, MBBS[1]; Bradley Porter, MBBS[1]; Julian Bostock, PhD[5]; Steven Niederer, PhD[1]; Reza Razavi, MBBS[1]; Christopher A. Rinaldi, MD[5]; Peter Taggart, MD, DSc[6]; Matthew Wright, PhD, FRCP, FHRS[5]; Jaswinder Gill, MD[5]

[1]Department of Imaging Sciences and Biomedical Engineering, King's College London, London; [2]INSIGNEO Institute for in-silico medicine, University of Sheffield, Sheffield, United Kingdom; [3]Boston Scientific Corp., St. Paul, MN; [4]Na Holmolce Hospital, Prague, Czech Republic; [5]Guys and St Thomas' Hospital; [6]University College London, London, United Kingdom

Correspondence:

Dr Nicholas Child

Cardiology Department

Guys and St Thomas' Hospital

London. SE1 7EH

United Kingdom

Tel: +44 20 7188 7188

Fax: +44 20 71885442

Email nchild@hotmail.com.

Journal Subject Terms: Arrhythmias; Atrial Fibrillation; Electrophysiology; Mechanisms

Abstract:

Background: The mechanisms that initiate and sustain persistent atrial fibrillation are not well characterised. Ablation results remain significantly worse than in paroxysmal atrial fibrillation in which the mechanism is better understood and subsequent targeted therapy has been developed. The aim of this study was to characterise and quantify patterns of activation during AF using contact mapping.

Methods and Results: Patients with persistent atrial fibrillation (n=14, mean age 61±8 years, LVEF 59±10%) underwent simultaneous biatrial contact mapping with 64 electrode catheters. The atrial electrograms were transformed into phase and subsequent spatiotemporal mapping was performed to identify phase singularities (PS). PS were located in both atria but we observed more PS in the left atrium compared to the right atrium (LA 779 ± 302, RA 552 ± 235, p=0.015). Although some PS of duration sufficient to complete >1 rotation were detected, the maximum PS duration was only 1150ms, and the vast majority (97%) of PS persisted for too short a period to complete a full rotation. Whilst in selected patients there was evidence of PS local clustering, overall PS were distributed globally throughout both chambers with no clear anatomical predisposition. In a subset of patients (n=7) analysis was repeated using an alternative established atrial PS mapping technique, which confirmed our initial findings.

Conclusions: No sustained rotors or localized drivers were detected, and instead the mechanism of arrhythmia maintenance was consistent with the multiple wavelet hypothesis, with passive activation of short-lived rotational activity.

Clinical Trial Registration: clinicaltrials.gov; Unique Identifier: NCT01765075

Key words: arrhythmia (mechanisms); atrial fibrillation; atrial fibrillation arrhythmia; mapping

Introduction

Atrial Fibrillation (AF) is the most common cardiac arrhythmia, affecting over 30 million individuals worldwide[1]. In addition, the overall worldwide incidence, prevalence and AF associated mortality is increasing[1]. Whilst incidence is higher in the elderly, the burden of AF is found throughout the entire adult population and results in major morbidity, mortality[2], and healthcare costs[3]. Despite the clear global impact of AF, our current understanding of the underlying disease process and mechanism of the arrhythmia remains substantially less than other common cardiac arrhythmias.

Paroxysmal AF (PAF) is a source based arrhythmia[4], whereas the mechanism of persistent AF (PsAF) is poorly understood and is based around sources, multiple wavelets and possibly rotors. There are inherent difficulties in mapping AF which contribute to this lack of understanding, and multiple different complex techniques being reported, yielding conflicting results. Our lack of understanding of the mechanisms underlying the initiation and maintenance of PsAF limits our ability to develop truly effective ablative therapies and is reflected by substantially lower success rates than in PAF[5]. The development of a unifying arrhythmia mechanism that can be used to target specific individual therapies in PsAF remains elusive in cardiac electrophysiology.

The aim of this study was to further understand the predominant mechanism that sustains PsAF in the human heart. We hypothesised that that there would be reproducible electrical mechanisms that would explain the maintenance of the atrial arrhythmia, and that these would be identifiable using phase analysis techniques.

Methods

In order to minimize the possibility of unintentionally sharing information that can be used to identify individuals, the raw data used in this study are not available. However, the analysis tools that support the findings of this study are available from the corresponding author upon reasonable request.

Study design and recruitment

The STARLIGHT study (NCT01765075) was a non-randomized multi-centre observational study to collect and analyse whole-chamber panoramic intracardiac electrograms immediately preceding cardiac ablation for PsAF. Patients were included in the study if they were due to undergo a clinically indicated ablation procedure for the treatment of PsAF. The main exclusion criteria were standard clinical AF ablation contraindications and additional criteria in which basket catheters may be associated with increased clinical risk, including the presence of permanent pacemaker leads, severely stenotic tricuspid and mitral valves and other abnormal atrial anatomy which would not be suitable for the Constellation™ catheters (Boston Scientific, St Paul, Minnesota, size 48, 60 and 75mm). Enrolment occurred in 2 European centers (Guys and St Thomas' Hospital, London and Na Homoice Hospital, Prague) between 5/28/13 and 12/31/2013. Class I and class III antiarrhythmic medications were withheld for 5 days prior to ablation, whilst amiodarone was continued. All patients gave informed consent and the study was approved by the local ethics committee. Table 1 summarises the clinical characteristics of each patient.

Data collection

Simultaneous biatrial panoramic recordings of unfiltered atrial electrograms were performed with 64-pole Constellation™ basket catheters prior to AF ablation. The atria were sized pre-

procedure for optimum catheter size using on-table echocardography. Following transeptal puncture IV heparin was infused to achieve activated clotting times of >350 seconds. The catheters were fully expanded in each atria, verified by fluoroscopy and transoesophageal echocardiography, and repositioned if necessary to ensure maximum coverage and contact electrodes. The atrial electrograms were visually inspected to ensure a high proportion of good quality electrograms, and redeployed if not.

Recordings were taken during baseline AF (presenting or induced), using the Ensite™ Velocity cardiac mapping system (St. Jude Medical) using 2 CathLink modules (providing a total of 128 electrode inputs) (Figure 1C, 1D). In patients presenting in sinus rhythm (representing persistent AF patients having undergone recent cardioversion) AF was initiated using rapid atrial pacing manoeuvres in keeping with recent similar study techniques[6]. Electrograms were recorded continuously for 10 seconds at a sampling rate of 2000 Hz (Figure 1). Patients then proceeded to their clinical AF ablation using standard techniques.

Data processing

Electroanatomical data (unipolar electrograms and their associated 3-dimensional (3D) co-ordinates, in addition to anatomical shells and surface electrograms) were exported and processed using Matlab (Mathworks, Natick, USA). The atrial electrograms then required a series of processing steps to transform them into phase in order to allow spatiotemporal mapping. These steps are summarized below and shown in Figure 2.

The timing of each ventricular beat was identified from reference coronary sinus electrograms (Figure 2B) using threshold crossing. An average ventricular beat was then calculated for each of the atrial electrodes by extracting signal segments with a duration equal to the average cycle length, aligned so that the start of the window preceded the timing of the

ventricular beat by 0.3 of the average cycle length. The average ventricular beat was then subtracted from each atrial signal. To remove power line interference and low frequency components, the atrial signals were then filtered with a 4th order Butterworth band pass filter with passband from 1 to 30 Hz, applied in forward and reverse mode so as to minimise phase distortion[7]. The dominant frequency of the electrogram at each electrode was identified from signal spectra obtained using the Welch method. Briefly, the 10 s recordings were divided into 4 epochs, each overlapping the preceding epoch by half its length. Each epoch was windowed with the Hanning function, and the fast Fourier transform of each windowed epoch was used to create an averaged spectrum with a frequency resolution of 0.25 Hz. The dominant frequency was then the frequency corresponding to the largest spectral peak.

Signals with low amplitude or exhibiting significant electrical noise were removed from the analysis and replaced with the average of signals recorded at the nearest neighbours in the basket (representing 0.2% of left atrium (LA) electrodes and 0.8% of right atrium (RA) electrodes).

Filtered signals were then recomposed using a method described previously[8] to produce a signal suitable for phase analysis. The recomposed signals were then interpolated for each 8 x 8 grid of electrodes using linear interpolation onto a new grid of 36 x 40 where each electrode was separated from its neighbour by 4 interpolated points, and included interpolation between spline 1 and spline 8 of the catheter system (Figure 2C). The alignment of the interpolated grid within the LA and RA anatomy is shown in Figure 2.

The interpolated and recomposed signals were transformed into phase by calculating the Hilbert transform of each signal, producing a phase map (Figure 2D). Phase singularities and wavefronts were then calculated using methods described previously[9,10].

In each frame, location of each phase singularity was compared with locations in the previous frame (10 ms earlier). Phase singularities separated by a threshold distance of ≤4 points on the interpolated grid were considered to be identical, and so we were able to estimate not only phase singularity lifetimes, but also the number of rotations supported by each phase singularity.

Subset validation of phase mapping technique

In a subset of patients analysis was repeated using an alternative previously tested method of phase analysis in AF to confirm the validity of our main phase mapping technique in cases of atrial tachycardia (n=3), longer lasting PS (n=2) and short lived PS (n=2). This analysis method has previously been extensively described [11], and further methodology specific to this study is presented in the supplemental methods.

Statistical Analysis

Statistics were performed using SPSS statistics, version 21 (IBM SPSS, New York). Results are reported as mean ± standard deviation. A paired T test was used to compare continuous variables. Correlation was explored through Person correlation and a p value of <0.05 was considered significant.

Results

Recruitment

Recordings from 14 patients were analysed (mean age 61±8 years, mean duration of PsAF 20.2±6.7 months, LVEF 59±10%, LA size 46 x 58mm, RA size 42 x 55mm). 5 patients had hypertension, 3 had treated obstructive sleep apnoea and 7 patients had a BMI>30 kg/m^2. Baseline demographics are presented in Table 1. Two patients had previously undergone AF ablations and 1 patient was on amiodarone. The mean duration of PsAF was 36 months. 8

patients presented in SR in whom AF was induced prior to mapping by rapid pacing. Basket catheters were successfully positioned in the left atrium (LA) and right atrium (RA) of each patient and basket sizes are shown in table 1.

Dominant frequency

The mean dominant frequency recorded over all 64 electrodes in the RA and LA is shown in Table 2. Overall, there was no significant difference between LA and RA dominant frequency.

Identification of phase singularities

In Figure 3, we illustrate a single phase singularity (PS) which was present for 0.93s, showing snapshots of recomposed voltage and phase, as well as the raw electrograms from four electrodes surrounding the phase singularity location. These electrograms are consistent with sequential depolarisation around the phase singularity, followed by regular activity as the phase singularity moves away from this quartet of electrodes.

Number of phase singularities

We identified PS in both atria, and the total number of PS detected in each atrium for each patient over the 10 s recording period is shown in Table 3. Over all 14 patients, the total number of PS detected in the LA over the 10 s analysis period was higher than the number detected in the RA (779 ± 302 vs 552 ± 235, $p = 0.015$). To compensate for differences in the catheter deployment, we calculated the total area covered by each basket. The number of PS per unit area is also given in Table 3, and as for the uncorrected numbers, the PS density was higher in the LA compared to the RA (0.166 ± 0.11 PS/mm^2 vs 0.07±0.04 PS/mm^2, $p = 0.002$).

Lifetime of phase singularities

Overall, there were more PS in the LA compared to the RA, but PS detected in the RA tended to have a longer lifetime (Mean lifetime RA 45.9 ± 22.0 ms, LA 38.4 ± 17.1 ms, p=0.009). Figure

4A shows a histogram of PS lifetimes in the LA and RA, indicating fewer short-lived PS in the RA compared to the LA. Figure 4B shows that the fraction of PS with lifetimes longer than 200 ms was higher in the RA compared to the LA (RA mean 3.77%, LA mean 2.74%, p=0.023).

However, the number of PS with lifetimes longer than 200 ms was small; in the LA we found 262 PS with lifetime longer than 200 ms, and 14 with a lifetime longer than 500 ms. In the RA we found 224 PS with a lifetime longer than 200 ms, and 19 with a lifetime longer than 500 ms. One patient had no PS in either RA or LA with a lifetime longer than 200 ms, and one further patient had no PS with a lifetime longer than 200 ms in the LA, but has two PS with a lifetime longer than 200 ms in the RA. The longest lasting PS in the entire cohort had a lifetime of only 1150 ms and represented 8.6 rotations. The percentage of PS persisting for more than 2 rotations was 2.6% in the LA and 2.5% in the RA.

LA and RA PS lifetime were strongly correlated (Pearson Correlation (PC) 0.95, $p<0.001$).

Location and clustering of phase singularities

The position of each PS was initially mapped onto an 8x8 2-dimensional array. This was then converted to a 3-dimensional reconstruction based on the 3D co-ordinates of each electrode. There was significant heterogeneity in the geometric distribution of PS distribution with some patients showing clustering of PS locations and others demonstrating a much more uniform distribution of PS spread throughout the atrium (Supplemental Figure 1). PS distribution was calculated for three sequential ten second recordings to assess the effects of recording duration on results of this study. Supplemental Figure 2 shows that PS distribution is similar across sequential recordings for a case with a more clustered distribution (mean correlation coefficient of 0.84), and a more uniform distribution (mean correlation coefficient of 0.86).

Anatomical location of phase singularities

There were no long lasting PS (longest PS duration 1150ms) so there is no merit on commenting on likely anatomical positions of rotors. PS were distributed globally throughout both chambers with no clear anatomical predisposition, irrespective of PS duration length (Figure 5).

Atrial size

LA short axis size was significantly correlated with PS lifetime duration (p=0.01), max PS lifetime duration (PC 0.70, p=0.005), and mean number of rotations (PC 0.59, p=0.025). RA short axis was not associated with any PS/rotation parameters. These results were not related to the size of the basket used.

Validity: comparison with an alternative AF mapping technique

Post hoc datasets were subjected to repeat analysis using an alternative AF phase mapping technique[11], assessed in the following categories: organized atrial tachycardia (n=3), longer lasting PS duration (n=2) and shorter PS duration (n=2). The atrial tachycardia group consists of one patient who presented and was mapped in left atrial tachycardia (and was subsequently excluded from our main results for PsAF), and two patients who presented in AF and developed atrial tachycardia during the ablation procedure.

Phase mapping of atrial tachycardia cases showed agreement across the different phase mapping techniques and to the activation patterns reported during the clinical cases. Figure 6A demonstrates an atrial tachycardia in which there was re-entry around the mitral valve annulus and passive right atrial activation, which was observed using both phase mapping techniques. This can be seen on the phase maps shown in anteroposterior 3D view, and the 2D displays of the left atrium for the original phase mapping methodology and the alternative method. Supplemental movies 1 & 2 show phase mapping of this tachycardia using the second method.

Longer lasting PSs identified using the original technique were also identified using the alternative technique. An example is shown in Fig 6B in which a drifting rotor is observed in the RA using both methods. Electrograms around the identified PS show sequential activation, with a large delay between the second and third electrograms as the PS trajectory covers a large area before activation reaches the third and fourth electrodes. Mean PS duration for recordings with longer lasting PS under the original method were also high under the alternative method (original method: mean 75.1 ± 21.5ms, alternative method: mean 59.9 ± 4.1ms, paired t-test for means does not show significant difference at 0.05 level: p=0.21), compared to recordings with shorter lasting PS under the original method (original method: 27.3 ± 3.52 ms, alternative method: 36.7 ± 8.3 ms, paired t-test does not show significant difference: p=0.08). Number of PS with lifetime > 100ms were also similar between the two techniques (longer lasting cases: original method mean 140 PS; alternative method mean 148 PS; shorter lasting cases: method 1 mean 37 PS; method 2 mean 71 PS).

In all the cases, the findings of our main phase analysis were confirmed with the alternative technique.

Discussion

The main finding from this study is that despite using whole-chamber panoramic endocardial mapping and a sophisticated analysis method no sustained rotors or localized drivers were identified in our PsAF cohort. Only very transient rotational activation was present, which by definition does not represent sources but likely the result of passive activation. This is despite using a comparable technique to that used previously by our group in successfully identifying

rotors during ventricular fibrillation. The PS results are consistent with the multiple wavelet hypotheses, and clearly in contrary to the rotor hypothesis.

Short-lived PS were identified in the majority of patients, reflecting the anatomical and functional electrical heterogeneities present in PsAF. However, such short-lived PS are not thought to play a role in sustaining AF, but secondary to passive activation. There was a greater density of PS in the LA compared to the RA, and also in larger left atriums, likely due to increased electrical and anatomical remodelling. LA and RA PS lifetime was also strongly correlated suggesting that the same underlying process is occurring in both atria. PS duration was shorter in the LA than the RA, possibly due to increased wavefront collisions. PS were found throughout all areas of each respective chamber, in a seemingly random distribution.

Despite substantial cellular, animal and human studies in PsAF the underlying mechanism responsible for initiation and perpetuating the condition remains non-defined and controversial. The importance of triggers originating from the pulmonary veins are well recognised, and underlie the basis for pulmonary vein isolation in PAF[4]. However, in PsAF the atria myocardium is thought to play an important role and there are 2 main contrary hypotheses to explain the underlying mechanism; namely the multiple wavelet hypothesis[12] and the currently favoured localized source hypothesis in which organized re-entrant circuits (rotors) or focal impulses disorganize into AF[13].

Previous studies have yielded conflicting results as to the presence of rotors. Traditionally the favoured mechanism underlying PsAF was the multiple wavelet hypothesis, in which AF was perpetuated by several randomly wandering wavefronts that vary in position, number and size[12]. This theory has been substantiated by a number of mapping studies from animals and humans[14,15], and recent body surface mapping studies[16].

Over recent years the alternative hypothesis of localised sources, and in particular rapidly activating atrial re-entrant circuits (rotors) as the mechanism for maintaining AF has been strongly advocated[17]. A substantial body of evidence is emerging substantiating this hypothesis using a variety of methodological techniques[18-21]. In the CONFIRM study rotors and localised focal sources were present in almost all of their AF patients (98%, mean 2.3 +/- 1.1 concurrent rotors and focal sources) and that targeting these local areas with ablation can terminate the arrhythmia and lead to improved clinical outcomes[13,22]. Yet despite such strong results, other research groups have failed to collaborate the high prevalence and stability of rotors[16,23,24], even whilst using datasets analysed using different sophisticated mapping techniques using datasets previously thought to show rotors in the CONFIRM study[25].

A rotor in mathematical terms is generally defined as a phase singularity in which the phase activation progresses through a complete cycle from $-\pi$ to $+\pi$. A rotor is also defined by a PS that persists for long enough for the phase pattern to cycle at least twice[26], whilst in the clinical studies many rotors are reported as stable over at least 30 minutes (thereby comprising thousands of rotations)[19]. Phase tracks progression of an area of myocardium through the action potential and is a thoroughly validated technique[27].

There are significant difficulties in mapping AF which underlie both the complex signal analysis required, and also possibly the conflicting results reported by different research groups. AF electrograms are very challenging to analyse due to fractionation, varying cycle lengths, and complex activation patterns, which result in difficulty assigning activation times and windows when assigning isochronal maps, and hence unlike atrial tachycardias are not suitable for clinical activation mapping. Removal of the ventricular signal from atrial electrograms can also be problematic[28], and poor quality signals can arise if an electrode is not in good contact with

excitable tissue. By converting the signals into phase, spatiotemporal mapping can be performed without the need to assign activation timings or windows, and the centre of rotational activation is clearly identified (phase singularities[11]). Despite phase analysis being the preferred method in mapping AF there are significant challenges in this approach due to the non-sinusoidal and fractionated nature of the recorded signal. A number of complex signal transformations and analytical methods have been used in response to these difficulties reporting conflicting results, and there is urgent need to validate and standardise these techniques.

This study utilised the approach reported by Kuklik et al, which recomposes the atrial electrogram from sinusoidal wavelets with amplitudes proportional to the negative slope of the electrogram[8]. This same approach in AF has recently been validated against the FIRM technique, in a small study (n=12) in which similar rotational activity was identified[29]. In order to map phase with the FIRM technique individual fibrillatory waves are substituted for unipolar action potential data using a previously validated library, which have a morphology more suited to the Hilbert transformation[29].

There are a number of similarities between our mapping and signal analysis method and the technique performed in the CONFIRM study, in that both studies used Constellation™ basket catheters[22], in order to achieve high density mapping and one would predict the same degree of inter electrode signal interpolation. There are a number of technical considerations and difficulties involved with mapping AF in this way, which has previously been reported by our group[30], and would have been similar across studies.

An alternative method by Roney et al, which was used in our mapping technique comparison substudy, applies a variety of filters to the electrogram signal to create a more sinusoidal signal, together with a pseudo-empirical mode decomposition to create a zero mean

signal, suitable for phase mapping. This has previously been validated and shown to perform well against simulated, experimental and clinical data in atrial tachycardia and AF, with the additional benefit of being able to use bipolar data, which is less susceptible to noise artefact[11]. In the mapping technique substudy we repeated our analysis using the alternative technique, in patients with an atrial tachycardia, relatively longer lasting PS and only very short PS duration. Both methods yielded very similar results, which whilst accepting this was only performed in a proportion of the patients is reassuring in terms of the scientific validity of our chosen main approach.

Our observations on the electrophysiology of atrial fibrillation are in contrast to our previous observations on ventricular fibrillation in humans[9]. In these studies VF was maintained by large coherent wavefronts interrupted by disorganised wavelet patterns. The conclusion from these studies was that human VF was driven by both mother rotor and multiple wavelet mechanisms. In the present study on atrial fibrillation evidence for rotor activity was minimal or absent. The explanation for these differences is at present unclear. Similar analytical methods were used in both studies. One possibility might be that the thicker walled ventricular myocardium is more favourable to the formation and stability of rotors than the thinner walled atrium.

Limitations

Limitations of this study include a relatively small number of patients with PSAF, however this should still represent a large enough cohort to have demonstrated rotors given their previously reported near universal incidence[13]. There are significant methodological differences between our method of data processing and phase transformation compared to the previously reported mechanism[13]. However, our process used a mathematically robust method, previously validated

in VF and atrial electrograms[8,9], and has been demonstrated to show short-lived rotational atrial activity (Figure 3). The electrogram sampling method is very similar to previous studies, using the same catheters and electroanatomic mapping systems[13], albeit in the new Topera system (Abbot Electrophysiology, CA, USA) there are some minor changes in electrode spacing. Other Intracardiac catheters may offer a higher density of electrodes but these will not allow whole chamber panoramic mapping. Previous studies have shown that basket catheters have sufficient resolution to detect rotors in human AF, but may result in a number of false PS detections that were not seen in simulations with double the number of splines[30], as such future catheter design could focus on basket catheters with an increased number of splines. Certainly equatorial bunching resulting in a range of inter-electrode spacing and difficulties with full electrode contact was observed in our cohort as previously described[31]. This is a universal problem with all studies and makes signal analysis more complex. We have not attempted to assess how the process of ablation will affect the electrical wavefronts in this paper. Additional limitations of our approach include the interpolation between electrodes, which were sometimes bunched, and the removal of poor quality signals.

Conclusion

No long-lasting rotors or localized drivers were found in this cohort of PSAF. Whilst relatively short-lived PS were identified, given their short lifespan these are likely secondary to passive activation, and not a mechanism for maintaining PSAF. We conclude therefore that the predominant mechanism in PSAF is the multiple wavelet hypotheses.

Sources of Funding: This was an industry sponsored and funded study by Boston Scientific. We acknowledge financial support from the Department of Health via the National Institute for Health Research (NIHR) Comprehensive Biomedical Research Centre award to Guy's and St

Thomas' NHS Foundation Trust in partnership with King's College London and King's College Hospital NHS Foundation Trust. RC is supported by an EPSRC grant EP/K037145/1. NC, JG and BP are both supported by an educational grant from St Jude Medical. CAR receives grants from St Jude Medical, Linanova, Medtronic and Boston Scientific.

Disclosures: Professor Gill is in receipt of a nonrelated grant from SJM. The other authors report no conflicts. Dr. Laughner, Dr. Shome, and Mr. Shuros are paid employees of Boston Scientific Corp

References:

1. Chugh SS, Havmoeller R, Narayanan K, Singh D, Rienstra M, Benjamin EJ, Gillum RF, Kim YH, McAnulty JH, Zheng ZJ, Forouzanfar MH, Naghavi GA, Mensah GA, Ezzati M, Murray CJ. Worldwide epidemiology of atrial fibrillation: a Global Burden of Disease 2010 Study. *Circulation*. 2014;129:837-47.

2. Benjamin EJ, Wolf PA, D'Agostino RB, Silbershatz H, Kannel WB, Levy D. Impact of atrial fibrillation on the risk of death: the Framingham Heart Study. *Circulation*. 1998;98:946-52.

3. Sheikh A, Patel NJ, Nalluri N, Agnihotri K, Spagnola J, Patel A, Asti D, Kanotra R, Khan H, Savani C, Arora S, Patel N, Thakkar B, Patel N, Pau D, Badheka AO, Deshmukh A, Kowalski M, Viles-Gonzalez J, Paydak H. Trends in Hospitalization for Atrial Fibrillation: Epidemiology, Cost, and Implications for the Future. *Prog Cardiovasc Dis*. 2015;58:105-16.

4. Haissaguerre M, Jais P, Shah DC, Takahashi A, Hocini M, Quiniou G, Garrigue S, Le Mouroux A, Le Metayer P, Clementy J. Spontaneous initiation of atrial fibrillation by ectopic beats originating in the pulmonary veins. *N Engl J Med*. 1998;339:659-66.

5. Calkins H, Kuck KH, Cappato R, Brugada J, Camm AJ, Chen SA, Crijns HJ, Damiano RJ, Davies DW, DiMarco J, Edgerton J, Ellenbogen K, Ezekowitz MD, Haines DE, Haissaguerre M, Hindrinks G, Lesaka Y, Jackman W, Jalife J, Jais P, Kalman J, Keane D, Kim YH, Kirchof P, Klein G, Kottkamp H, Kumagai K, Lindsay BD, Mansour M, Marchlinski FE, McCarthy PM, Mont JL, Morady F, Nademanee K, Nakagawa H, Natale A, Nattel S, Packer DL, Pappone C, Prystowsky E, Raviele A, Reddy V, Rushkin JN, Shemin RJ, Tsao HM, Wilber D. 2012 HRS/EHRA/ECAS Expert Consensus Statement on Catheter and Surgical Ablation of Atrial Fibrillation: recommendations for patient selection, procedural techniques, patient management and follow-up, definitions, endpoints, and research trial design. *Europace*. 2012;14:528-606.

6. Narayan SM, Krummen DE, Clopton P, Shivkumar K, Miller JM. Direct or coincidental elimination of stable rotors or focal sources may explain successful atrial fibrillation ablation: on-treatment analysis of the CONFIRM trial (Conventional ablation for AF with or without focal impulse and rotor modulation). *J Am Coll Cardiol*. 2013;62:138-47.

7. Bradley CP, Clayton RH, Nash MP, et al. Human ventricular fibrillation during global ischemia and reperfusion: paradoxical changes in activation rate and wavefront complexity. *Circ Arrhythm Electrophysiol*. 2011;4:684-91.

8. Kuklik P, Zeemering S, Maesen B, Maessen J, Crijns HJ, Verheule S, Ganesan AN, Schotten U. Reconstruction of instantaneous phase of unipolar atrial contact electrogram using a concept of sinusoidal recomposition and Hilbert transform. *IEEE Trans Biomed Eng*. 2015;62:296-302.

9. Nash MP, Mourad A, Clayton RH, Sutton PM, Bradley CP, Hayward M, Patterson DJ, Taggart P. Evidence for multiple mechanisms in human ventricular fibrillation. *Circulation*. 2006;114:536-42.

10. Clayton RH, Nash MP. Analysis of cardiac fibrillation using phase mapping. *Card Electrophysiol Clin*. 2015;7:49-58.

11. Roney, CH, Cantwell CD, Qureshi NA, Chowdhury RA, Dupont E, Lim PB, Vigmond EJ, Tweedy JH, Ng FS, Peters N. Rotor Tracking using Phase of Electrograms Recorded during Atrial Fibrillation. *Ann Biomed Eng*. 2017;45:910-923

12. Moe GK, Rheinboldt WC, Abildskov JA. A Computer Model of Atrial Fibrillation. *Am Heart J*. 1964;67:200-20.

13. Narayan SM, Krummen DE, Shivkumar K, Clopton P, Rappel WJ, Miller JM. Treatment of atrial fibrillation by the ablation of localized sources: CONFIRM (Conventional Ablation for Atrial Fibrillation With or Without Focal Impulse and Rotor Modulation) trial. *J Am Coll Cardiol*. 2012;60:628-36.

14. Allessie MA, Bonke FI, Schopman FJ. Circus movement in rabbit atrial muscle as a mechanism of tachycardia. II. The role of nonuniform recovery of excitability in the occurrence of unidirectional block, as studied with multiple microelectrodes. *Circ Res*. 1976;39:168-77.

15. Cox JL, Canavan TE, Schuessler RB, Cain ME, Lindsay BD, Stone C, Smith PK, Corr PB, Boineau JP. The surgical treatment of atrial fibrillation. II. Intraoperative electrophysiologic mapping and description of the electrophysiologic basis of atrial flutter and atrial fibrillation. *J Thorac Cardiovasc Surg*. 1991;101:406-26.

16. Cuculich PS, Wang Y, Lindsay BD, Faddis MN, Schuessler RB, Damiano RJ, Li L, Ruddy Y. Noninvasive characterization of epicardial activation in humans with diverse atrial fibrillation patterns. *Circulation*. 2010;122:1364-72.

17. Vaquero M, Calvo D, Jalife J. Cardiac fibrillation: from ion channels to rotors in the human heart. *Heart Rhythm*. 2008;5:872-9.

18. Ganesan AN, Kuklik P, Lau DH, Brooks AG, Baumert M, Lim WW, Thanigaimani S, Nayyar S, Mahajan R, Kalman JM, Roberts-Thomson KC, Sanders P. Bipolar electrogram

shannon entropy at sites of rotational activation: implications for ablation of atrial fibrillation. *Circ Arrhythm Electrophysiol*. 2013;6:48-57.

19. Skanes AC, Mandapati R, Berenfeld O, Davidenko JM, Jalife J. Spatiotemporal periodicity during atrial fibrillation in the isolated sheep heart. *Circulation*. 1998;98:1236-48.

20. Kalifa J, Tanaka K, Zaitsev AV, Warran M, Vaidanathan R, Auerbach D, Pandit S, Vikstrom KL, Ploutz-Snyder R, Talkachou A, Atienza F, Guiraudon G, Jalife J, Berenfeld O. Mechanisms of wave fractionation at boundaries of high-frequency excitation in the posterior left atrium of the isolated sheep heart during atrial fibrillation. *Circulation*. 2006;113:626-33.

21. Haissaguerre M, Hocini M, Denis A, Shah AJ, Komatsu Y, Yamashita S, Daly M, Amraoui S, Zellerhoff S, Picat MQ, Quotb A, Jesel L, Lim H, Ploux S, Bordachar P, Attuel G, Meillet V, Ritter P, Derval N, Sacher F, Bernus O, Cochet H, Jais P, Dubois R. Driver domains in persistent atrial fibrillation. *Circulation*. 2014;130:530-8.

22. Narayan SM, Baykaner T, Clopton P, Schricker A, Lalani GG, krummen DE, Shivkumar K, Miller JM. Ablation of rotor and focal sources reduces late recurrence of atrial fibrillation compared with trigger ablation alone: extended follow-up of the CONFIRM trial (Conventional Ablation for Atrial Fibrillation With or Without Focal Impulse and Rotor Modulation). *J Am Coll Cardiol*. 2014;63:1761-8.

23. Lee G, Kumar S, Teh A, Madry A, Spence S, Larobina M, Goldblatt J, Brown R, Atkinson V, Moten S, Morton JB, Sanders P, Kistler PM, Kalman JM. Epicardial wave mapping in human long-lasting persistent atrial fibrillation: transient rotational circuits, complex wavefronts, and disorganized activity. *Eur Heart J*. 2014;35:86-97.

24. Lin YJ, Lo MT, Lin C, Chang SL, Lo LW, Hu YF, Hsieh WH, Chang HY, Lin WY, Chung FP, Liao JN, Chen YY, Hanafy D, Huang NE, Chen SA. Prevalence, characteristics, mapping, and catheter ablation of potential rotors in nonparoxysmal atrial fibrillation. *Circ Arrhythm Electrophysiol*. 2013;6:851-8.

25. Benharash P, Buch E, Frank P, Share M, Tung R, Shivkumar K, Mandapati R. Quantitative analysis of localized sources identified by focal impulse and rotor modulation mapping in atrial fibrillation. *Circ Arrhythm Electrophysiol*. 2015;8:554-61.

26. Umapathy K, Nair K, Masse S, Krishnan S, Rogers J, Nash MP, Nanthakumar K. Phase mapping of cardiac fibrillation. *Circ Arrhythm Electrophysiol*. 2010;3:105-14.

27. Gray RA, Pertsov AM, Jalife J. Spatial and temporal organization during cardiac fibrillation. *Nature*. 1998;392:75-8.

28. Salinet JL, Madeiro JPV, Cortez PC, Stafford P, Ng AG, Schlindwein FS. *Med Biol Eng Comput*. 2013;51: 1381.

29. Alhusseini M, Vidmar D, Meckler GL, Kowalewski CA, Shenasa F, Wang PJ, Narayan SM,

Rappel WJ. Two Independent Mapping Techniques Identify Rotational Activity Patterns at Sites of Local Termination During Persistent Atrial Fibrillation. *J Cardiovasc Electrophysiol*. 2017;28;6:615-622.

30. Roney CH, Cantwell CD, Bayer JD, Qureshi NA, Lim PB, Tweedy JH, Kanagaratnam P, Peters NS, Vigmond EJ, Ng FS, Spatial Resolution Requirements for Accurate Identification of Drivers of Atrial Fibrillation, *Circ Arrhythm Electrophysiol*. 2017;19;5:

31. Laughner J, Shome S, Child N, Shuros A, Neuzil P, Gill J, Wright M. Practical Considerations of Mapping Persistent Atrial Fibrillation with Whole-Chamber Basket Catheters. *JACC Clin Electrophysiol*. 2016;2;1:55-65.

Table 1. Baseline demographics

Study no	Age (years)	Gender	EF	NYHA	Prior atrial ablation	Outcomes at 30 days	LA size (mm)	LA Basket (mm)	RA size (mm)	RA Basket (mm)
1	51	Female	55	2	No	SR	43x52	48	38x50	48
2	75	Male	39	2	No	AFl	45x43	48	33x44	48
3	61	Male	41	1	No	SR	61x51	60	72x43	60
4	45	Male	63	1	No	SR	45x45	48	46x46	48
5	63	Male	71	1	No	SR	56x45	60	55x42	60
6	59	Male	74	1	No	SR	51x40	48	50x40	48
7	59	Male	65	3	No	SR	65x48	60	56x52	60
8	50	Male	58	1	No	SR	56x42	60	55x38	60
9	68	Male	60	1	No	SR	61x39	60	49x34	48
10	68	Female	60	1	No	AF	75x48	60	64x49	60
11	61	Male	60	1	No	AFl	65x47	60	62x46	60
12	56	Male	55	1	Yes	AF	55x45	60	53x39	48
13	75	Male	67	2	Yes	SR	61x53	60	57x44	60
14	63	Male	60	2	No	Junctional	64x54	60	63x43	60

EF – Ejection Fraction, NYHA – New York Heart Association heart failure score, LA - left atrium, RA - right atrium, SR – sinus rhythm, AFl – atrial flutter, AF – atrial fibrillation

Table 2: Dominant frequency recorded in each patient.

Patient	**LA dominant frequency (Hz)**		**RA dominant frequency (Hz)**	
	Mean	**SD**	**Mean**	**SD**
1	5.531	1.383	4.922	0.523
2	5.094	0.428	5.086	0.309
3	3.812	0.367	4.684	2.803
4	6.973	3.587	7.309	4.586
5	5.262	1.564	4.672	0.704
6	5.352	0.862	5.102	0.556
7	4.539	0.349	4.879	0.846
8	9.195	2.71	12.828	4.097
9	3.523	0.599	3.422	0.35
10	6.492	2.085	6.531	2.725
11	6.457	0.207	5.953	0.609
12	6.004	0.618	5.406	0.749
13	4.59	0.303	4.746	0.444
14	4.477	0.61	4.523	0.617
Overall	5.5215		5.718785714	

Table 3: Number and duration of phase singularities detected in each patient over each 10 s analysis period.

Pt no	LA				RA			
	No. of PS	PS / area (mm^{-2})	PS > 200 ms	Max rotations	No. of PS	PS / area (mm^{-2})	PS > 200 ms	Max rotations
1	1232	0.20	9	2.04	686	0.06	22	6.23
2	950	0.17	3	2.19	775	0.14	4	2.05
3	441	0.05	3	2.55	564	0.04	10	2.02
4	733	0.29	0	1.48	1151	0.16	2	3.43
5	666	0.16	10	1.81	534	0.05	12	2.54
6	1014	0.44	10	1.87	752	0.12	18	4.87
7	910	0.31	39	3.42	366	0.06	10	3.11
8	389	0.12	0	0.71	475	0.07	0	0.94
9	544	0.11	59	5.83	327	0.05	50	5.54
10	206	0.06	13	2.87	203	0.05	13	3.13
11	897	0.15	12	3.02	515	0.05	12	6.16
12	1211	0.13	19	3.61	568	0.06	20	5.30
13	908	0.08	45	3.98	433	0.03	33	10.09
14	813	0.05	40	3.77	386	0.04	18	3.94
Mean	779	0.17	18.7	2.80	552	0.07	16	4.24

Figure Legends:

Figure 1. Deployment, recording and mapping from biatrial Constellation™ basket catheter: A – left atrium venogram in the anterior posterior (AP) projection. B – Constellation™ basket catheters (Boston Scientific, Natick, MA, USA) deployed in both atria simultaneously (coronary sinus catheter and ablation catheters also present) in the AP projection. C – 64 simultaneous electrograms recorded from a single constellation catheter to deliver high-density AF electrograms. D - 3D visualization of the same catheters within the anatomical shell using Velocity.

Figure 2. Transformation of atrial electrograms to phase: A – The recording electrodes are located in 3D geometry. B – The atrial electrograms undergo a series of filters and are recomposed (described in more detail in the main text). C – The recomposed signals are interpolated into the 8x8 grid and subsequent 3D locations. S1-S2 denote spline locations, and 8 denotes location of distal electrode 8 on spline S1. D – The Hilbert transformation is then used to construct phase maps for the recomposed data.

Figure 3. Example of a short-lived Phase Singularity (lasting 0.93 seconds): A- Raw electrode signals recorded at locations E1-E4. Blue box indicates the time interval highlighted in C and D, red arrow shows sequential activation at E1-E4, and green line shows lifetime of re-entry. B- Anatomical landmarks for interpolated grid shown in C and D. C- Snapshots of recomposed electrode voltage, showing phase singularities (green: circles anticlockwise, squares clockwise), and wavefronts (blue). Grey boxes show location of electrodes E1-E4. D- Snapshots

of phase corresponding to recomposed voltage in C.

Figure 4. Phase singularity results: A - Histogram of phase singularity lifetimes in left atrium (red) and right atrium (red). B - Percentage of phase singularities in left atrium (red) and right atrium (blue) with lifetime longer than 200 ms.

Figure 5. **Anatomical location of rotors in LA (left) and RA (right) regions:** Each bar shows the number of PS detected over a 10 s period in each anatomical location, normalised by the number of electrodes and summed over all 14 patients. The bar colours indicate PS with lifetime more than 200 ms (blue), between 100 and 200 ms (red), and less than 100 ms (yellow).

Figure 6. Comparison of two different phase mapping techniques and validation in the case of atrial tachycardia: A - Atrial tachycardia dataset: Left: Snapshots of phase calculated using the alternative method (method 2) shown on the atrial shells in the anteroposterior view (top) posteroanterior view (bottom); Right: Phase mapping for the original method (method 1, top row) and alternative method (method 2, bottom row) for the left atrium and right atrium. White arrow indicates direction of wavefront propagation, where straight lines indicate reentry is observed around the mitral valve. B - Longer lasting PS dataset: Left: Snapshots of phase calculated using method 1 (top) and method 2 (bottom) for the left atrium and right atrium; Right: Electrode signals following QRS subtraction recorded at locations E1-E4. Blue box indicates the time interval centred on phase snapshots; red arrow shows sequential activation at E1-E4. Grey boxes show location of electrodes E1-E4

What is known?

- Atrial Fibrillation is most common cardiac arrhythmia, with an increasing incidence, and is a major cause of morbidity and mortality.
- Ablation of paroxysmal atrial fibrillation is substantially more successful than persistent atrial fibrillation (PsAF) and is thought to reflect our lack of understanding of the mechanism involved in PsAF.

What the study adds?

- Whilst phase singularities were frequently identified, these were all short lived and there was no evidence of sustained rotor activity.
- These results were consistent when repeated in a sub-study using an alternative rotor mapping technique.

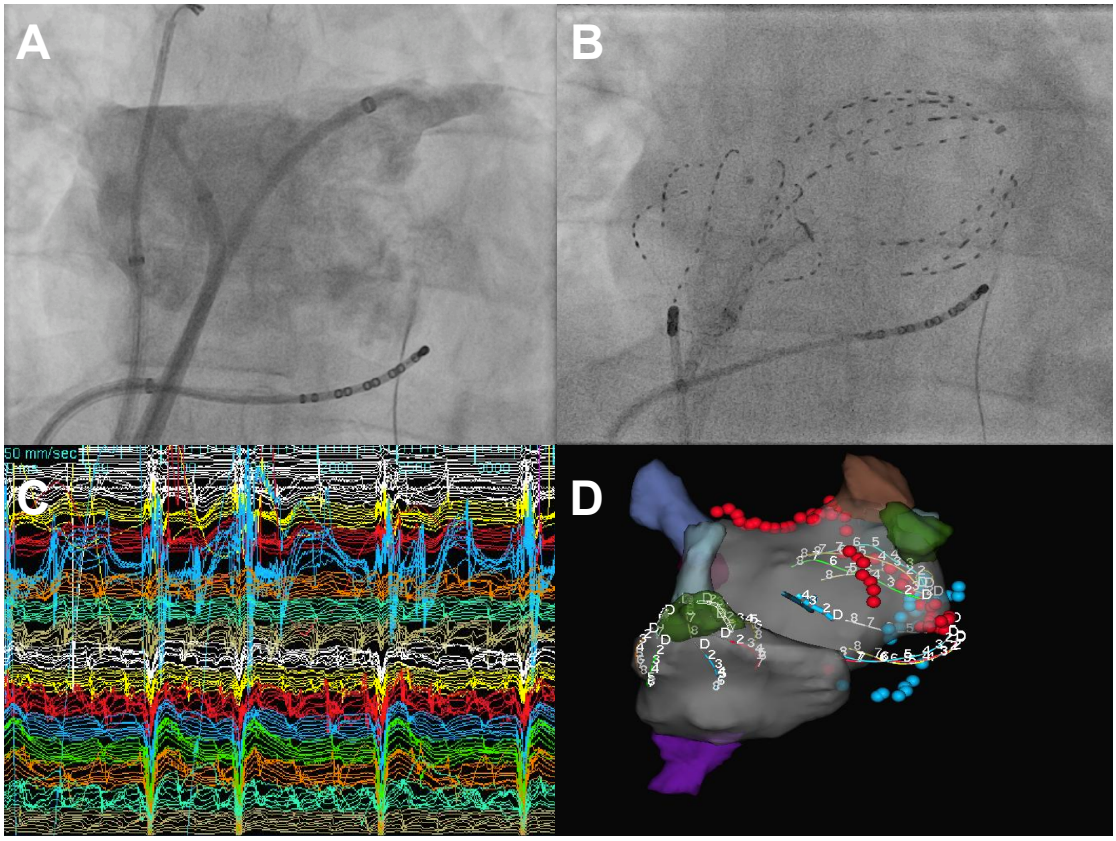
A
B
50 mm/sec
C
D

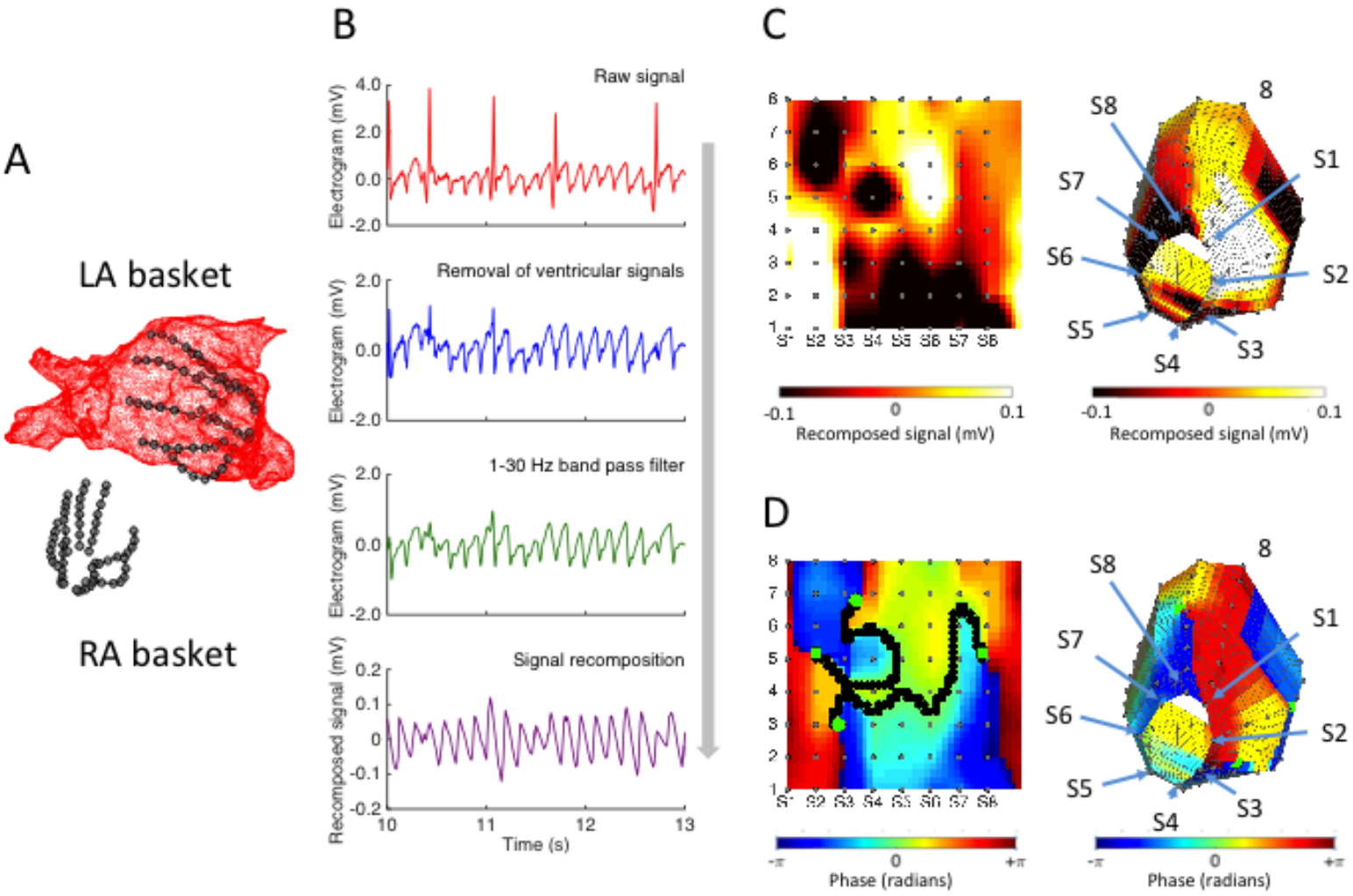
A
LA basket
RA basket
B
Raw signal
Electrogram (mV)
Removal of ventricular signals
Electrogram (mV)
1-30 Hz band pass filter
Electrogram (mV)
Signal recomposition
Recomposed signal (mV)
Time (s)
C
Recomposed signal (mV)
S8
S1
S7
S6
S2
S5
S3
S4
Recomposed signal (mV)
D
Phase (radians)
Phase (radians)

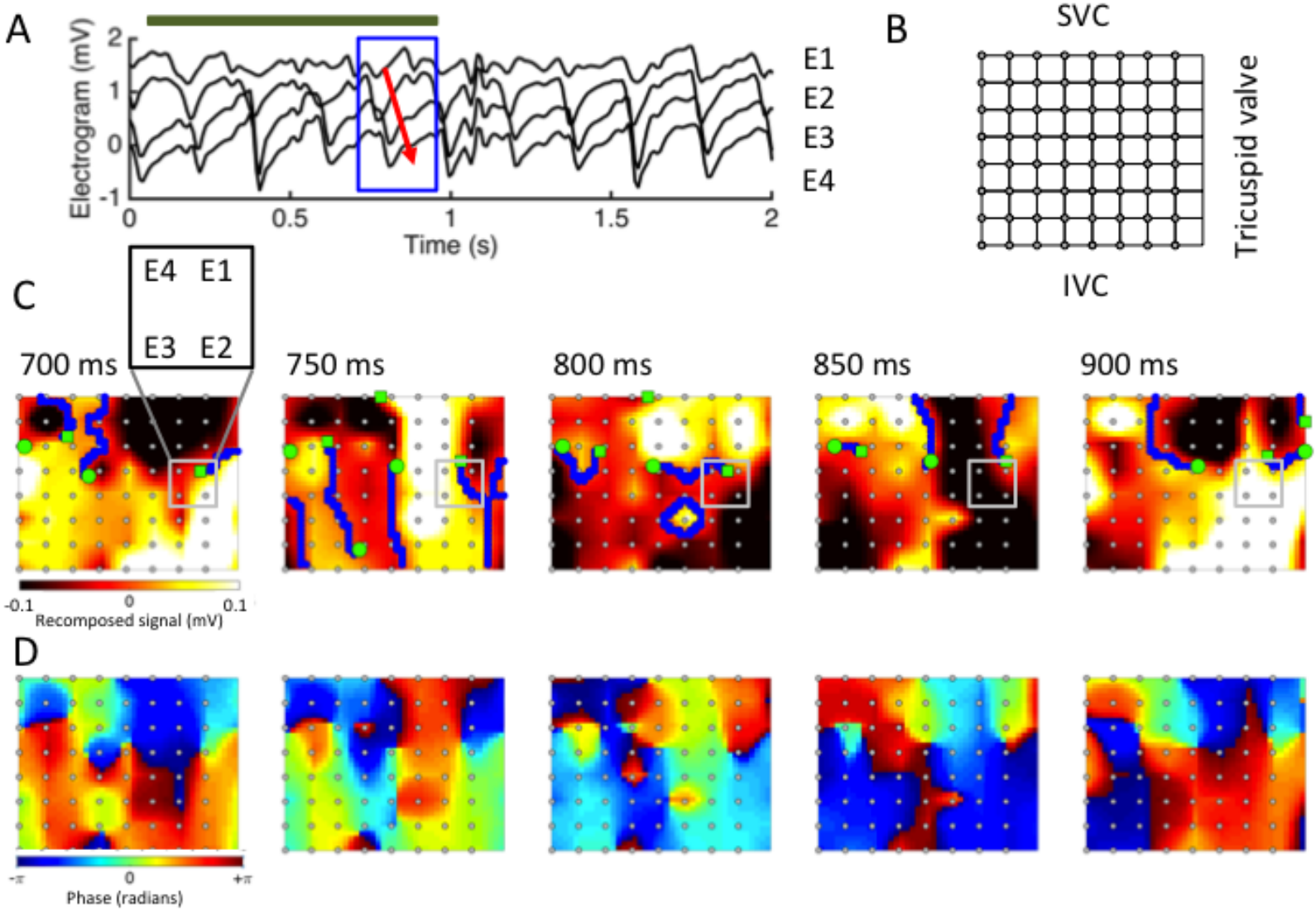
A
Electrogram (mV)
2
1
0
-1
0
0.5
1
1.5
2
Time (s)
E1
E2
E3
E4
B
SVC
Tricuspid valve
IVC
C
E4 E1
E3 E2
700 ms
750 ms
800 ms
850 ms
900 ms
-0.1
0
0.1
Recomposed signal (mV)
D
-π
0
+π
Phase (radians)

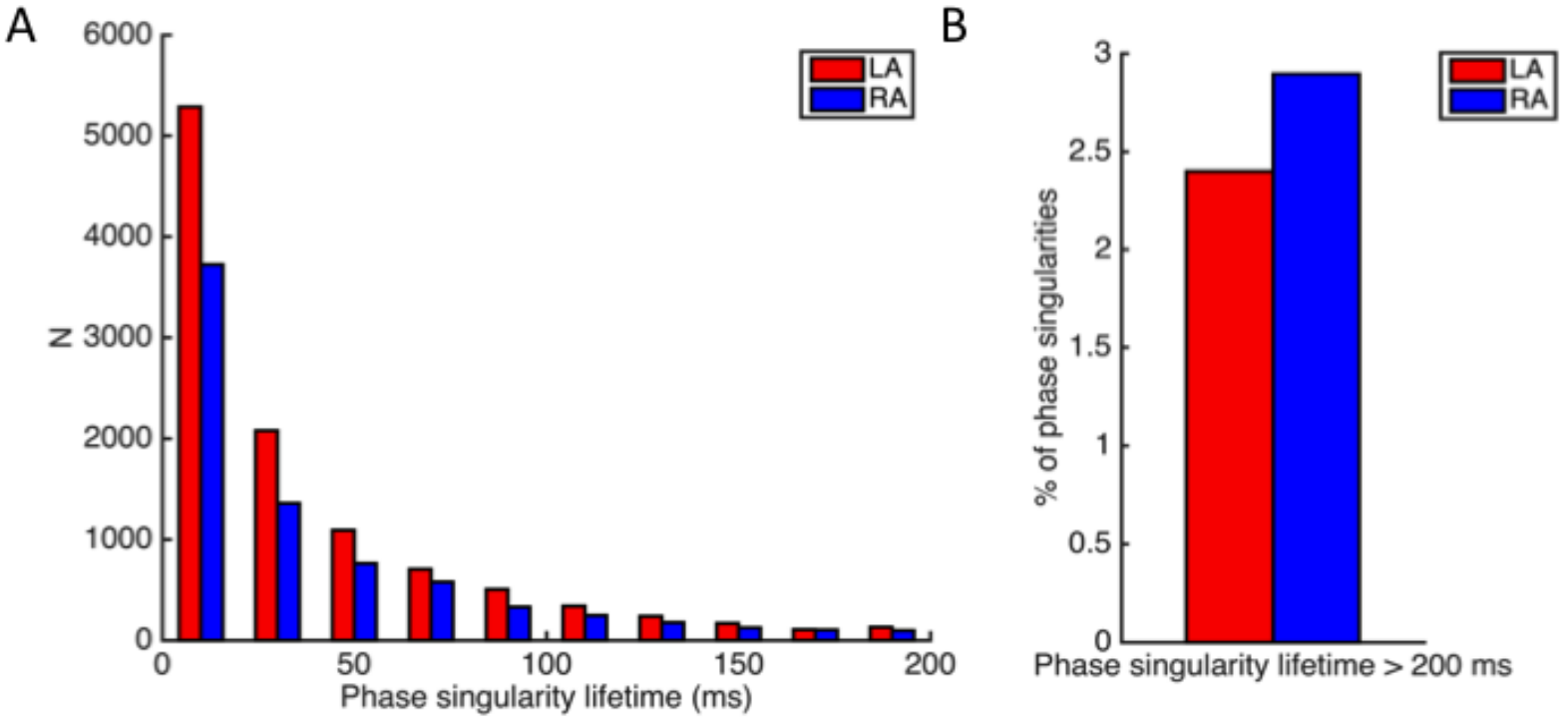
A
6000
5000
4000
3000
2000
1000
0
N
0
50
100
150
200
Phase singularity lifetime (ms)
LA
RA
B
3
2.5
2
1.5
1
0.5
0
% of phase singularities
Phase singularity lifetime > 200 ms
LA
RA

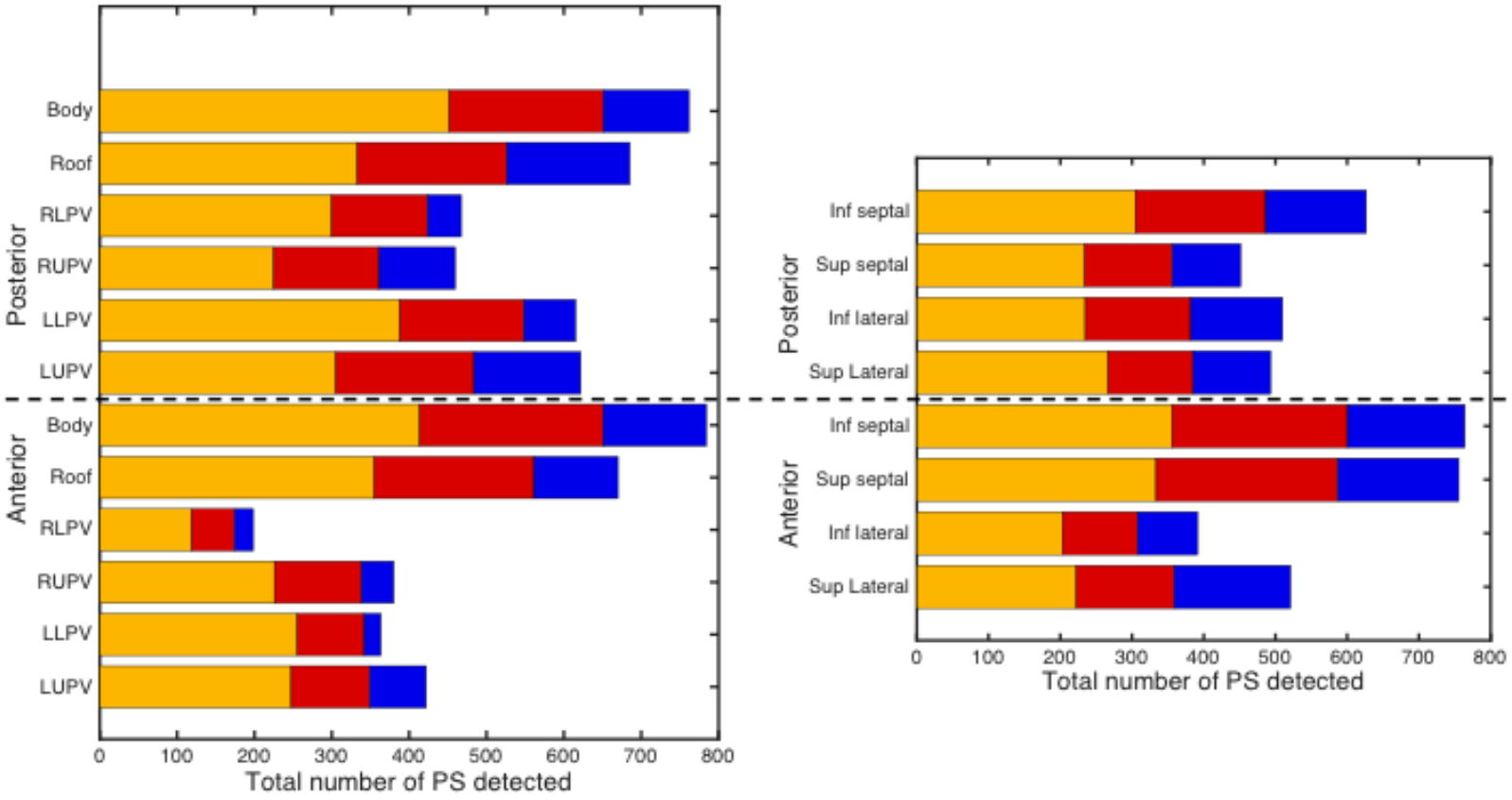
Posterior
Body
Roof
RLPV
RUPV
LLPV
LUPV
Anterior
Body
Roof
RLPV
RUPV
LLPV
LUPV
0
100
200
300
400
500
600
700
800
Total number of PS detected
Posterior
Inf septal
Sup septal
Inf lateral
Sup Lateral
Anterior
Inf septal
Sup septal
Inf lateral
Sup Lateral
0
100
200
300
400
500
600
700
800
Total number of PS detected

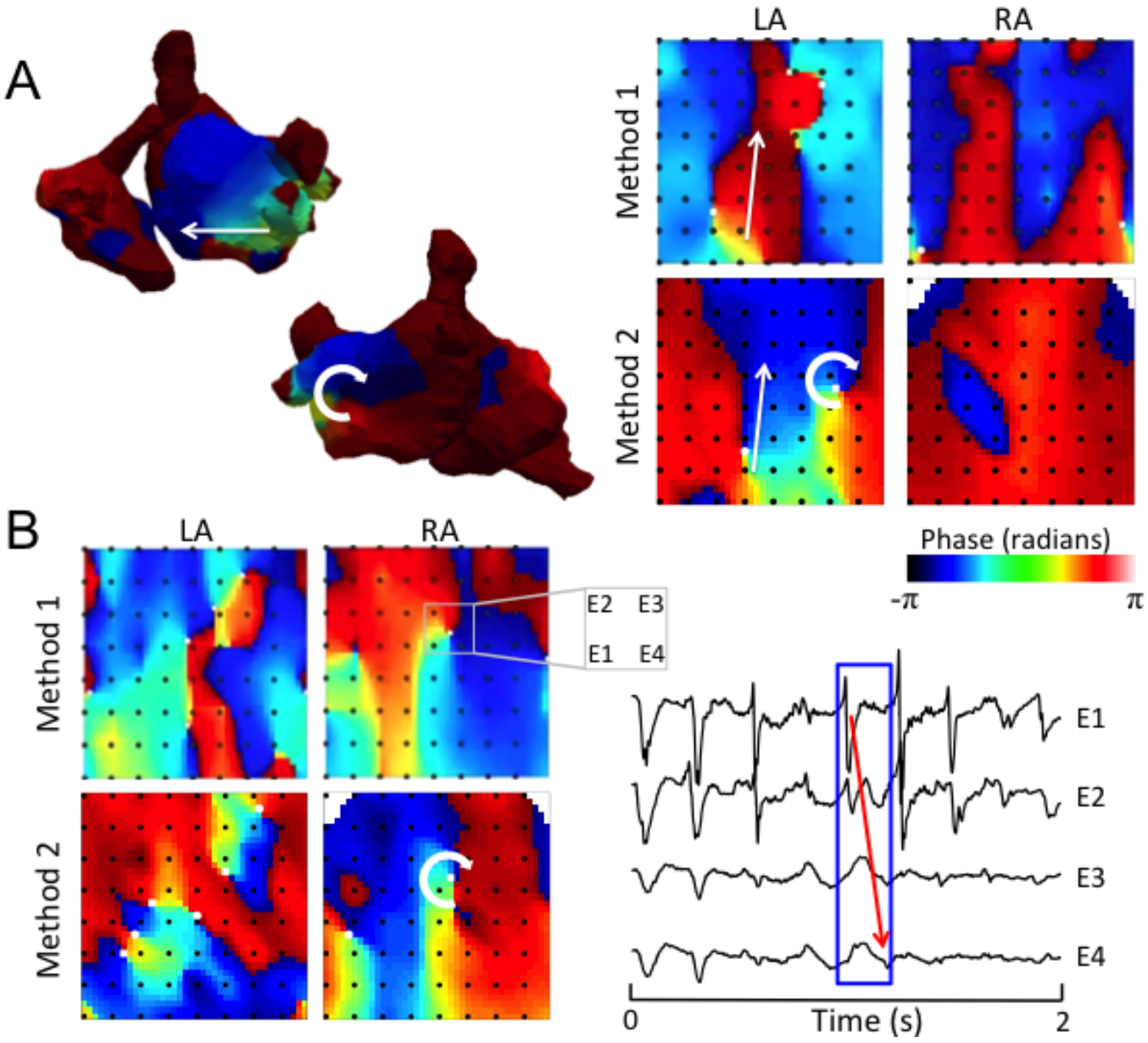
A
LA
RA
Method 1
Method 2
B
LA
RA
Method 1
Method 2
E2 E3
E1 E4
Phase (radians)
-π
π
E1
E2
E3
E4
0
Time (s)
2